44 KSME Journal, Vol. 2, No. 1, pp. 44~51, 1988.

LAMINAR FLUID FLOW IN A TWISTED ELLIPTIC TUBE

Keun-Shik Chang*, Jong-Soo Choi and Jae-Soo Kim*****

(Received March 8, 1988)

Twisted tubes are important in generating secondary flow and fluid mixing in a cross-stream direction. In the present paper, the fully developed laminar fluid flow through twisted elliptic tubes is numerically analyzed up to a large twist ratio by using the finite difference method. The elliptic solution domain is transformed to a rectangular computational domain by using a new, simple, and analytic transformation containing a removable singularity. The effect of the two parameters, the tube twist ratio and the aspect ratio of the ellipse, is investigated with respect to their role in determining the axial and circumferential velocities, the streamline patterns, and the resistance coefficients.

Key Words : Twisted Elliptic Tube, Fully-Developed Flow, Analytic Teansformation, Secondary Flow

NOMENCLATURE

a, b : Minor and major semi-axis of an ellipse, respectively
E : A prescribed error
f : Friction factor
H : Axial length of a twisted tube over a half rotation ($H = H^*/a$)
$\hat{i}$, $\hat{j}$, $\hat{k}$: Unit vector in x, y, z-coordinate direction
$l(y)$: The distance from the y-axis to the wall
$\vec{P}_g$: Pressure gradient vector (P_x, P_y, P_z)
Re : Reynolds number, $2a< V_z >/\nu$
$\hat{S}$: Unit vector along a curve on which x, y is fixed and z varies
$\hat{t}$: The inward unit vector normal to the tube wall
U_0 : Maximum axial velocity in Poiseuille flow
V_0 : Axial velocity in Poiseuille flow
$\vec{V}$: Velocity vector (V_x, V_y, V_z)
V'_x, V'_y : Relative velocity component with respect to the cross-section
W : Deviation of the axial velocity from the Poiseuille flow
x, y, z : Rotational Cartesian coordinates
$\bar{x}$, $\bar{y}$, $\bar{z}$: Fixed Cartesian coordinates
Q : Flow rate
ξ, η, ζ : Coordinates in the computation domain
$\vec{\omega}$: Vorticity vector ω_x, ω_y, ω_z
ψ : Stream function
ν : Kinematic viscosity
λ : Aspect ratio, b/a
α : Counter-clockwise angle from the x-axis
$\langle T_w \rangle$: Average equivalent shear stress

Superscripts

n : n-th iteration
$*$: Dimensional quantities

Subscripts

w : Wall values
b : Bulk mean values

Parenthesis

$\langle\ \rangle$: Averaged value

*Department of Mechanical Engineering, Korea Advanced Institute of Science and Technology, P.O. Box 150, Cheongryang, Seoul 130-650, Korea
**Ph. D. Student, Pennsylvania State University
***Korea Institute of Space Sciences and Astronomy

1. INTRODUCTION

Fluid flow through ducts of various cross-sectional shapes has been quite extensively studied in the literature due to its many engineering applications. Useful data on these duct flows obtained either theoretically or by experimental method are collected in the heat transfer handbook by Rohsenow and Hartnett (1973).

From an engineering point of view, ducts having good heat transfer rate with smaller wet perimeter and/or with the reduced power loss for a given mass flux are sometimes required. It has been known that the secondary flow can enhance heat transfer significantly in the curved part of a duct.

As a means of generating the secondary flows, twisted tubes have been considered in addition to curved ones. Lopina and Bergles (1969) made an experiment with a straight pipe having twisted tape inserted inside. Date (1974) solved numerically the identical problem using a finite-difference method. Todd (1977) investigated a rather general problem, the twisted tubes. He was able to simplify the Navier-Stokes equations with small twist ratio assumption in the rotating coordinates, which was solved by a regular perturbation method. He derived a fourth-order partial differential equation for the stream function and showed that it is identical to the equation for the small transverse displacement of a clamped elastic

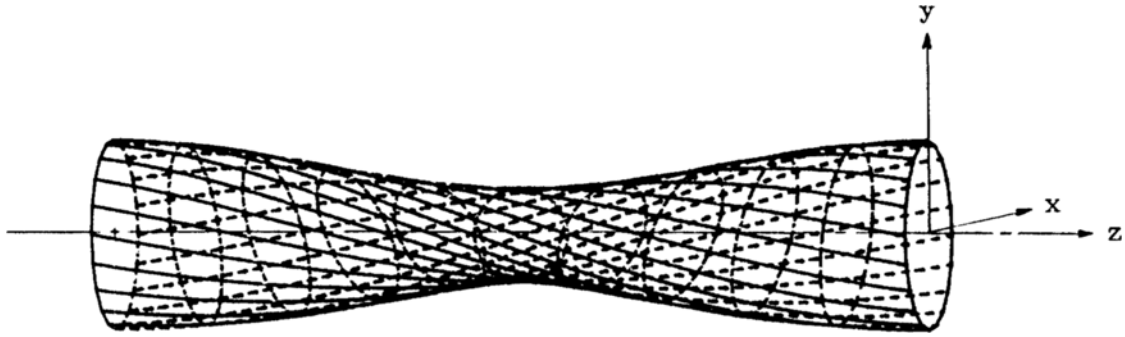

Fig. 1 Twisted elliptic tube

plate under a constant loading. His analysis is correct in principle for a pipe of any cross-section with proper boundary conditions, but its validity is limited only to a slightly twisted elliptic pipe.

In the present paper a fully developed laminar flow in a twisted elliptic tube (see Fig. 1) is investigated without the restriction of a small twist ratio. Three control parameters govern this problem: the pressure gradient in the axial direction, the pipe twist ratio and the aspect ratio (the ratio of the major axis to the minor axis) of the elliptic cross-section. To solve this problem numerically, the governing Navier-Stokes equations are first written in the rotating Cartesian coordinate system. A new simple transformation method is then applied to map the elliptic physical domain to a rectangular computational one, which can be in general applied to a duct of any cross-section. Validity of the present solution was demonstrated by its close proximity to the Todd's in a small-twist ratio limit. The parametric effects of the twist ratio and the cross-sectional aspect ratio have been investigated.

2. GOVERNING EQUATIONS AND TRANSFORMATION

The flow configuration under consideration is a twisted pipe having a straight center line and a rotating, elliptic cross-sectional geometry. Fully-developed viscous flow through this pipe is governed by the Navier-Stokes equations in a full three-dimensional space. However, they can be reduced to a two-dimensional form by using the rotating rectangular Cartesian coordinate system shown in Fig. 2 (Todd, 1977; Masliyah and Nandakumar, 1981a, 1981b). The

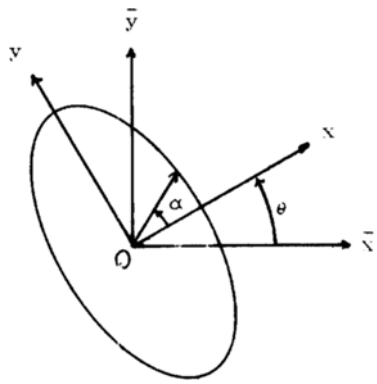

Fig. 2 Fixed and rotating Cartesian coordinates

dimensionless governing equations in the rotating coordinates are rather complicated and take the following form: continuity equation

$$\frac{\partial V_x}{\partial x}+\frac{\partial V_y}{\partial y}+\frac{\pi}{H}\left(y\frac{\partial V_z}{\partial x}-x\frac{\partial V_z}{\partial y}\right)=0 \tag{1}$$

x-direction momentum equation

$$\begin{aligned}&V_x\frac{\partial V_x}{\partial x}+V_y\frac{\partial V_x}{\partial y}+\frac{\pi}{H}V_z\left(y\frac{\partial V_x}{\partial y}-x\frac{\partial V_x}{\partial y}-V_y\right)\\&=-p_x+\frac{\partial^2 V_x}{\partial x^2}+\frac{\partial^2 V_x}{\partial y^2}+\left(\frac{\pi}{H}\right)^2\left(x^2\frac{\partial^2 V_x}{\partial y^2}+y^2\frac{\partial^2 V_x}{\partial x^2}\right.\\&\left.-2xy\frac{\partial^2 V_x}{\partial x\partial y}-y\frac{\partial V_x}{\partial y}-x\frac{\partial V_x}{\partial x}-V_x+2x\frac{\partial V_y}{\partial y}-2y\frac{\partial V_y}{\partial x}\right)\end{aligned} \tag{2}$$

y-direction momentum equation

$$\begin{aligned}&V_x\frac{\partial V_y}{\partial x}+V_y\frac{\partial V_y}{\partial y}+\frac{\pi}{H}V_z\left(y\frac{\partial V_y}{\partial y}-x\frac{\partial V_y}{\partial y}+V_x\right)\\&=-p_y+\frac{\partial^2 V_y}{\partial x^2}+\frac{\partial^2 V_y}{\partial y^2}+\left(\frac{\pi}{H}\right)^2\left(y^2\frac{\partial^2 V_y}{\partial x^2}+x^2\frac{\partial^2 V_y}{\partial y^2}\right.\\&\left.-2xy\frac{\partial^2 V_y}{\partial x\partial y}-y\frac{\partial V_y}{\partial y}-x\frac{\partial V_y}{\partial x}-V_y+2y\frac{\partial V_x}{\partial x}-2x\frac{\partial V_x}{\partial y}\right)\end{aligned} \tag{3}$$

z-direction momentum equation

$$\begin{aligned}&V_x\frac{\partial V_z}{\partial x}+V_y\frac{\partial V_z}{\partial y}+\frac{\pi}{H}V_z\left(y\frac{\partial V_z}{\partial x}-x\frac{\partial V_z}{\partial y}\right)\\&=-p_z-\frac{\pi}{H}(yp_x-xp_y)+\frac{\partial^2 V_z}{\partial x^2}+\frac{\partial^2 V_z}{\partial y^2}\\&+\left(\frac{\pi}{H}\right)^2\left(y^2\frac{\partial^2 V_z}{\partial x^2}+x^2\frac{\partial^2 V_z}{\partial y^2}-x\frac{\partial V_z}{\partial y^2}-y\frac{\partial V_z}{\partial y}\right.\\&\left.-2xy\frac{\partial^2 V_z}{\partial x\partial y}\right)\end{aligned} \tag{4}$$

In the above equations, all the gradients in the z-direction except the pressure terms are dropped due to the fully-developed flow assumption. A stream function which satisfies the continuity Eq. (1) is now defined as

$$\begin{aligned}\frac{\partial\psi}{\partial y}&=V_x+\frac{\pi}{H}yV_z\\\frac{\partial\psi}{\partial x}&=-V_y+\frac{\pi}{H}xV_z\end{aligned} \tag{5}$$

With the aid of the vorticity function defined by

$$\omega_z=\frac{\partial V_y}{\partial x}-\frac{\partial V_x}{\partial y} \tag{6}$$

the governing equations are recast as follows:

the stream function equation

$$\omega_z = -\frac{\partial^2\psi}{\partial x^2} - \frac{\partial^2\psi}{\partial y^2} + \frac{\pi}{H}\left(2V_z + x\frac{\partial V_z}{\partial x} + y\frac{\partial V_y}{\partial y}\right) \tag{7}$$

z-direction vorticity transport equation

$$\begin{aligned}&\frac{\partial\psi}{\partial y}\frac{\partial\omega_z}{\partial x} - \frac{\partial\psi}{\partial x}\frac{\partial\omega_z}{\partial y} + \omega_z\frac{\pi}{H}\left(x\frac{\partial V_z}{\partial y} - y\frac{\partial V_z}{\partial x}\right)\\ &+\frac{\pi}{H}\left(y\frac{\partial V_y}{\partial x} - x\frac{\partial V_y}{\partial y} + V_x\right)\frac{\partial V_z}{\partial x}\\ &-\frac{\pi}{H}\left(y\frac{\partial V_z}{\partial x} - x\frac{\partial V_x}{\partial y} - V_y\right)\frac{\partial V_z}{\partial y}\\ &=\frac{\partial^2\omega_z}{\partial x^2} + \frac{\partial^2\omega_z}{\partial y^2} + \left(\frac{\pi}{H}\right)^2\left(x^2\frac{\partial^2\omega_z}{\partial y^2}\right.\\ &\left.+y^2\frac{\partial^2\omega_z}{\partial x^2} - x\frac{\partial\omega_z}{\partial x} - y\frac{\partial\omega_z}{\partial y} - 2xy\frac{\partial^2\omega_z}{\partial x\partial y}\right)\end{aligned} \tag{8}$$

As a result, the governing equations now consist of Eqs. (4), (7) and (8). In solving the axial momentum equation, the pressure gradient in z-direction which is directly related to the Reynolds number must be specified as a parameter controlling the flow rate. However, once the solutions for the stream function and the vorticity are obtained, the local pressure gradient terms in other directions can be calculated from Eqs. (2) and (3).

It is important in any numerical method for a system of partial differential equations that the boundary conditions be specified on an exact boundary. The Cartesian coordinates are not appropriate for this purpose and thus a new general coordinate system is needed. A new simple coordinate transformation is now proposed as in Fig. 3, i. e.,

$$\begin{aligned}&\xi = \frac{x}{l(y)}\ ;\quad l(y) = \{1-(y/\lambda)^2\}^{\frac{1}{2}}\\ &\eta = y\\ &\zeta = z\end{aligned} \tag{9}$$

where $l(y)$ represents the distance from the y-axis to the tube wall. In this particular transformation, the vertex point A in Fig. 3 is singular in the sense that one physical point is mapped to multiple points in the computational domain. However, this singularity is numerically removable since it is located on a solid boundary where the flow data are single-valued and subject to the no-slip condition. The transformed governing equations now become very complicated in the computational domain (ξ, η, ζ) and are separately elaborated in the Appendix. The boundary conditions must now be respecified. On the wall,

$$\begin{aligned}&\psi = 0,\\ &V_z = 0,\\ &\omega_z = -\frac{\partial^2\psi}{\partial\eta^2} + \left(\frac{\pi}{H}\right)\eta\frac{\partial V_z}{\partial\eta} \qquad (\text{at } \eta=\lambda)\end{aligned} \tag{10}$$

and

$$\begin{aligned}\omega_z = &-\left\{\left(\frac{\partial\xi}{\partial x}\right)^2 + \left(\frac{\partial\xi}{\partial y}\right)^2\right\}\frac{\partial^2\psi}{\partial\xi^2}\\ &+\frac{\pi}{H}\left\{\xi l\left(\frac{\partial\xi}{\partial x}\right) + \eta\left(\frac{\partial\xi}{\partial y}\right)\right\}\frac{\partial V_z}{\partial\xi} \qquad (\text{at } \xi=-1,\ 1)\end{aligned}$$

Assuming antisymmetry of the pipe flow, we have on the x-axis $(\eta=0,\ 0<\xi<1)$,

$$\begin{aligned}&\psi(-\xi,\ 0) = \psi(\xi,\ 0)\\ &V_z(-\xi,\ 0) = V_z(\xi,\ 0)\\ &\omega_z(-\xi,\ 0) = \omega_z(\xi,\ 0)\end{aligned} \tag{11}$$

where $0<\xi<1$.

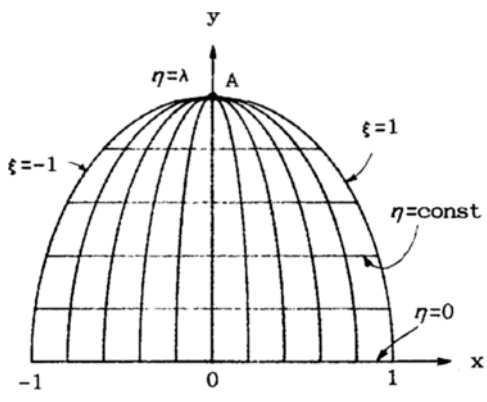

Fig. 3 Computational coordinate system

4. NUMERICAL METHOD

The complexity of the governing equations requires finite difference method as simple as possible to get the axial velocity, stream function, and vorticity. We employed the successive over-relaxation method after approximating all the derivative with second-order central difference schemes. The appropriate relaxation factor for the vorticity transport equation was found to be near the value 1.0.

The finite-difference solution did not converge well at high Reynolds numbers and high twist ratios if the initial flow data were poor. So, the case of small twist ratio was first solved and its data were used as an initial condition for the more twisted tubes. As H was decreased, optimal over-relaxation factors for both the stream-function and the axial velocity were also decreased from 1.7 to 1.2.

As one can see from Fig. 3, the singular point A or the maximum-η point $(\eta=\lambda)$ should have one and the same functional value for each unknown in the physical plane. However, in the numerical procedure the wall vorticity at the singular point evaluated by using Eq. (10) becomes widely varied depending on what constant-ξ line we choose to evaluate the necessary flow data. We used the data from the straight central axis, i.e., the $\xi=0$ line to evaluate the wall vorticity at the singular point A. This actually accelerated the convergence rate better than any other methods attempted.

Besides this removable singularity, other merits exist with the present body-fitted coordinates: denser mesh points are assigned in the region where the nearby wall has a large curvature. In addition, the present transformation is analytic and applicable to tubes of any general cross-section shape, eliminating numerical errors associated with the finite-differencing of the transformation metrics that would result in any other numerical mappings.

The iterative numerical procedure is first started by solving the finite-difference analog of Eq. (A-5) once, updating the vorticity at each interior point. Then, we move to Eq. (A-4) for the stream function and Eq. (A-3) for the axial veloc-

ity. Normally the number of local iteration needed to achieve convergence for the above two equation was increased up to five as H was decreased. To solve the axial-velocity Eq. (A-3), unknown pressure gradient terms p_x and p_y had to be calculated from Eqs. (A-1) and (A-2).

The above procedure constituted one complete overall cycle of iteration. After 200 to 500 overall iterations, the preassigned convergence criterion for the vorticity

$$E_\omega = \frac{Max \left| \omega_{i,j}^{(n)} - \omega_{i,j}^{(n-1)} \right|}{max \left| \omega_{i,j}^{(n)} \right|} \leq 5.0 \times 10^{-4} \tag{12}$$

was satisfied where the superscript (n) refers to the n-th iteration.

5. RESULTS AND DISCUSSION

Axial velocity of the Poiseuille flow in an untwisted straight elliptic tube has the paraboloidal contour

$$V_0(x, y) = U_0\left(1 - \frac{x^2}{a^2} - \frac{y^2}{b^2}\right) \tag{13}$$

which is shown in Fig. 4(a), where U_0 represents the maximum axial velocity equal to twice the flow rate Q. In Fig. 4(b) the axial velocity component is plotted for a twisted tube having the same flow parameter P_z. Distortion of the profile from the paraboloid is clearly visible. Deviation of the axial velocity from the paraboloidal Poiseuille flow can be expressed for a twisted tube by

$$W = V_z - V_0$$

Todd (1977) solved the fluid flow through a slightly twisted elliptic tube. He simplified transformed Navier-Stokes equations in the rotating coordinates by using the regular perturbation method. However, his results show streamlines and W-levels having symmetry with respect to both the x-and y-axis for all the twist ratios considered, which could not evidently be so for a realistic problem.

Comparison with Todd's analytic solution is presented in Fig. 5, in terms of the maximum relative percentage error in the stream function values. As can be observed from the curve, maximum error for $H=400$ lies within 4%, suggesting that Todd's solution is reasonable only for very small twist ratios.

Another comparison between the two methods, the present and the Todd's, is demonstrated in the iso-W lines in Fig. 6, which are obtained for the same flow and geometric parameters as in the above. Although the isolines from the present method are inclined slightly toward the right, they qualitatively agree well with the Todd's solution (Fig.6(a)) for the relatively small twist ratio ($H=400$). From this result we can safely assume that the present numerical solution is accurate and more general than Todd's.

The cross-flow velocity vectors from the present computation are shown in Fig. 7. To be able to analyze the viscous effect distinguished from the flow rotation due to the tube twist, however, we reformulate these velocity components in a more convenient way. Let $\hat{S}$ be a unit vector along a helical curve on which the coordinates (x, y) are fixed and z varies;

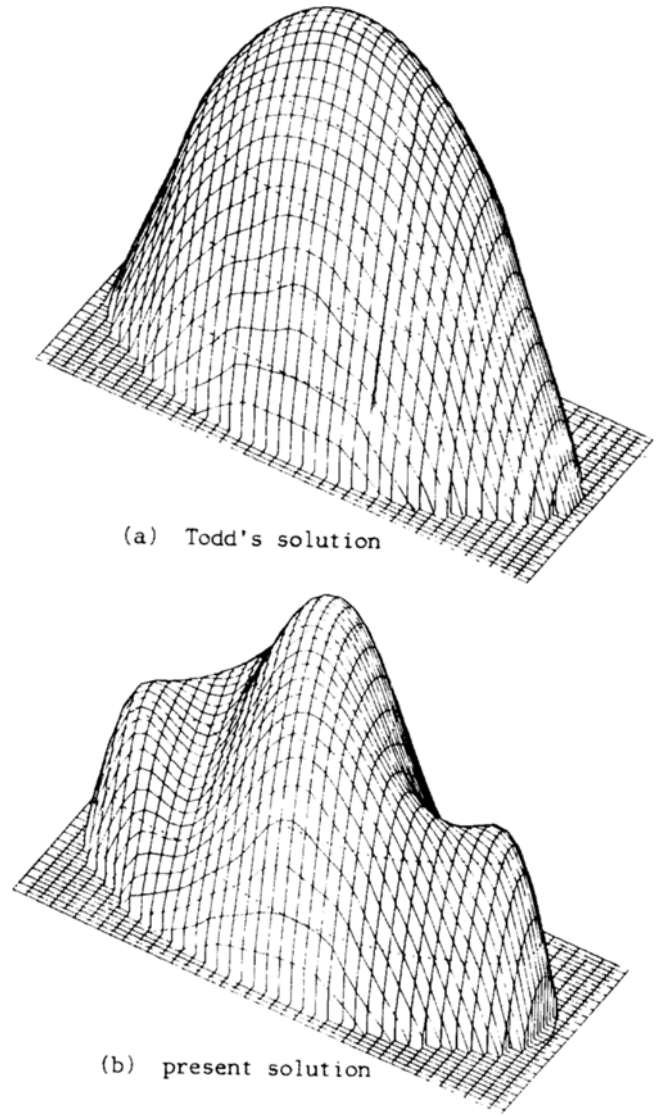

Fig. 4 Axial velocity profile in an elliptic tube ($\lambda=2.5$, $P_z=-1160$)

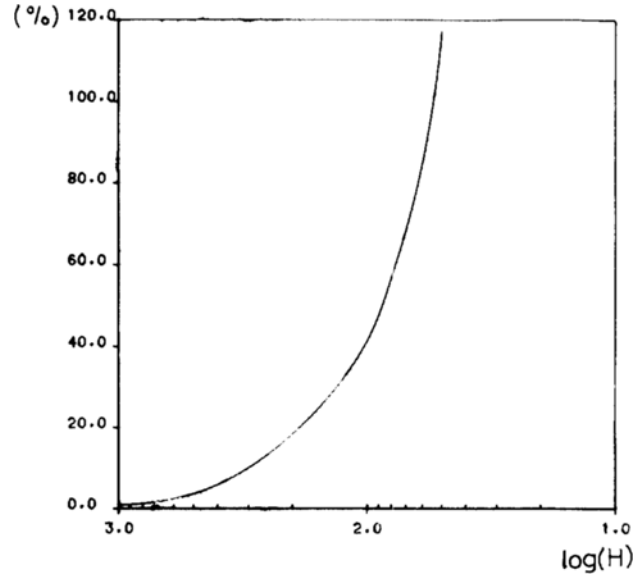

Fig. 5 Maximum error in the stream function values of the Todd's solution relative to the present

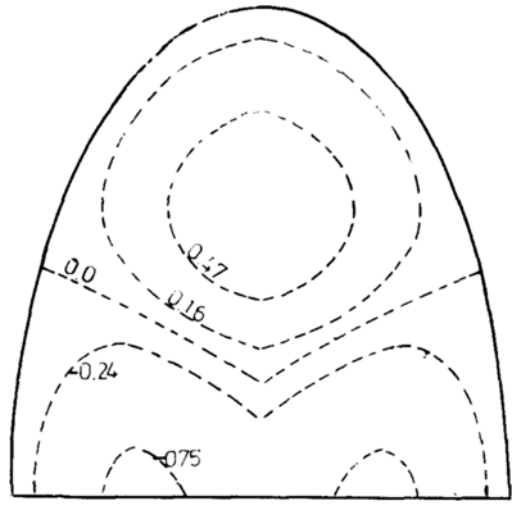

(a) Todd's solution

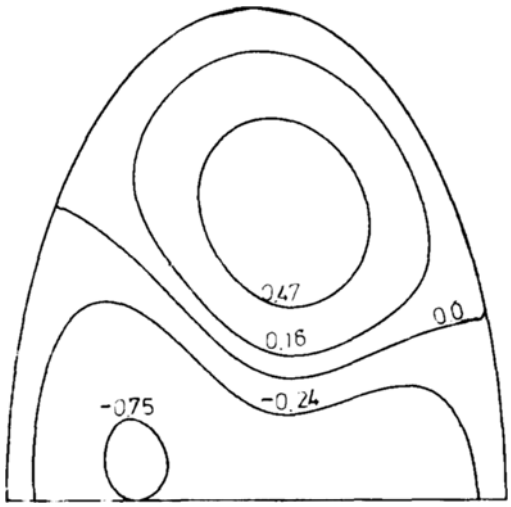

(b) present solution

Fig. 6 Iso-W contour lines for the same parameters (H=400)

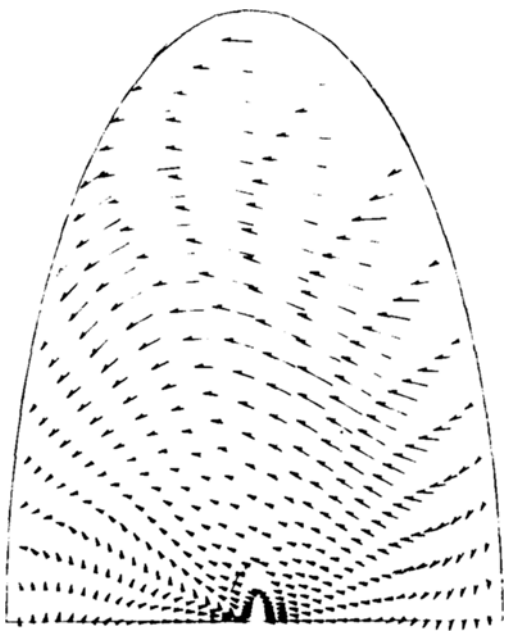

Fig. 7 Absolute cross-sectional velocity vectors (V_x, V_y) : $\lambda=2.5$, $P_z=-1160$, $Re=387$, $H=20$

this unit vector is pointing to the direction of increasing z. If a fluid particle had velocity vector directed to $\hat{S}$-direction, it would not change its relative position in the different cross-sections of the pipe. A careful examination reveals that it is the velocity difference

$$\vec{V}-\left\{\frac{V_z}{(\hat{k}\cdot\hat{S})}\right\}\hat{S}$$

that will cause the migration of a fluid particle relative to the pipe cross-section, see Masliyah and Nandakumar (1981b). Here,

$$\hat{S}=(\hat{k}-\frac{\pi}{H}y\hat{i}+\frac{\pi}{H}\times\hat{j})/\left\{1+\left(\frac{\pi}{H}\right)^2(x^2+y^2)\right\}^{\frac{1}{2}} \tag{15}$$

Then, the migration will be governed to a first approximation by the perturbed velocity having the components

$$\begin{aligned} V'_x &= V_x+\frac{\pi}{H}yV_z \\ V'_y &= V_y-\frac{\pi}{H}xV_z \end{aligned} \tag{16}$$

These new velocity components are caused by the viscous effect and are shown in Fig. 8 as a vector plot for the same flow conditions as in Fig. 7. Streamlines outlined by V'_x and V'_y are evidently helpful in figuring the secondary flow structures.

In order to see the effect of the twist ratio, distribution of the secondary flow velocity components scaled by U_0 is shown along the x-axis and y-axis in Fig. 9. Also presented is their stream function contours for different aspect ratios in Fig. 10. For the cases of large H or small aspect ratios, the secondary flow lags behind the winding motion of the potential flow in the twisted tube, as seen from Fig. 10. On the

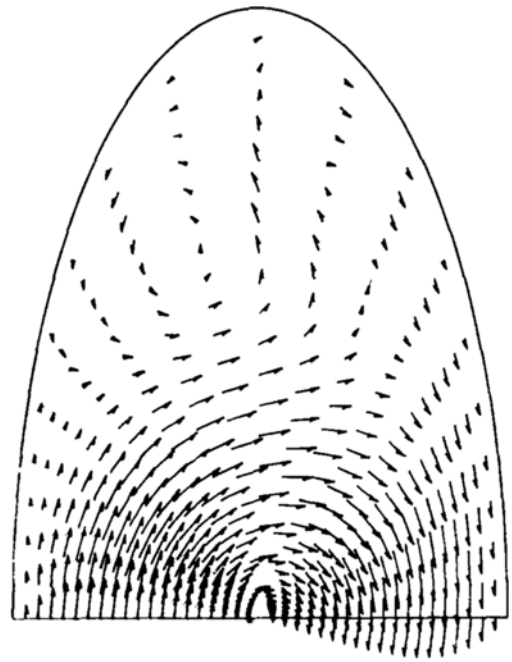

Fig. 8 Relative cross-sectional velocity vectors (V'_x, V'_y) : $\lambda=2.5$, $P_z=-1160$, $Re=387$, $H=20$

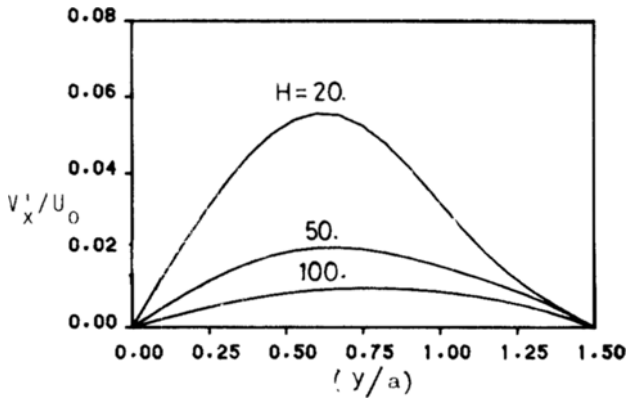

(a) V_x' on the y-axis

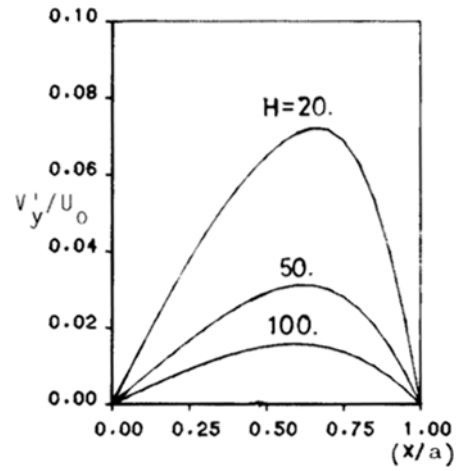

(b) V_y' on the x-axis

Fig. 9 Relative cross-sectional velocity profile on the x-and y-axis ($\lambda=1.5$)

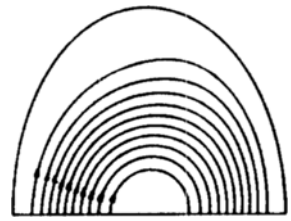

(a) $\lambda=1.5$, $P_z=-1444$, Re=478.01, H=20

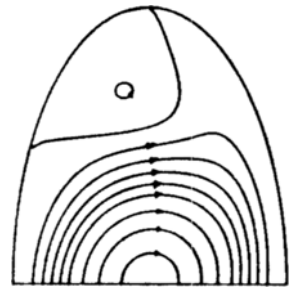

(b) $\lambda=2.0$, $P_z=-1250$, Re=424.15, H=20

(c) $\lambda=2.5$, $P_z=-1160$, Re=387.53, H=20

Fig.10 Contour of secondary stream function

contrary, for relatively small H or large aspect ratio, the secondary flow accelerates ahead of the twisting rate of the potential flow.

This phenomenon can also be viewed from the axial velocity distributions shown in Fig. 11 and 12. Due to the viscous rotating flow, larger centrifugal force is generated on the fluid particles in the direction of the major axis, but not near the wall. Its consequence is that a large positive radial pressure gradient is produced in the region where the nearby tube wall has large curvature. When a uniformly rotating potential flow is superposed on it, it is not difficult to envision that a strong secondary flow is resulted due to this circumferential pressure gradient, as observed from Fig. 7. The larger the aspect ratio of a tube is, the more influential this viscous secondary effect becomes. This phenomenon is directly related to the large degree of deviation of the axial velocity profile from the paraboloid for an elliptic tube of large aspect ratio.

Now, the friction factor f is defined by

$$f=\frac{\langle \tau_w^* \rangle}{\frac{1}{2}\rho \langle V_z^* \rangle^2} \tag{17}$$

where $\langle \tau_w^* \rangle$ is an average equivalent shear stress acting over

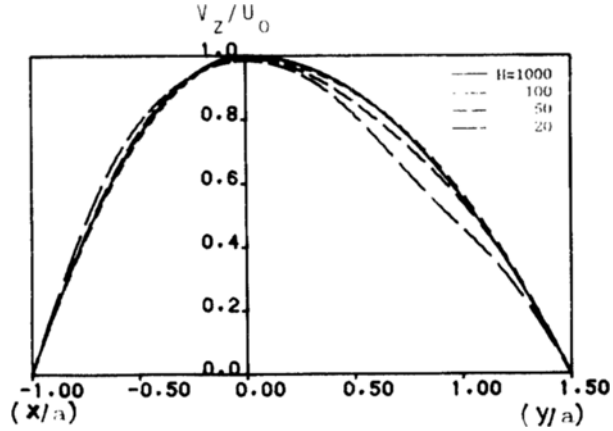

Fig.11 Axial velocity profile on the x-and y-axis ($\lambda=1.5$)

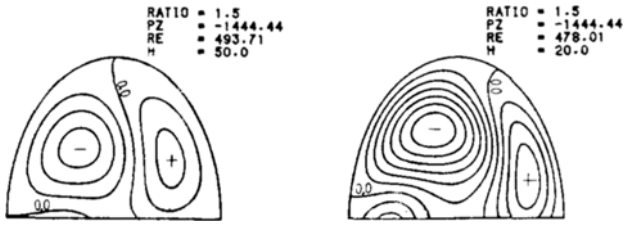

(a) Aspect ratio λ=1.5

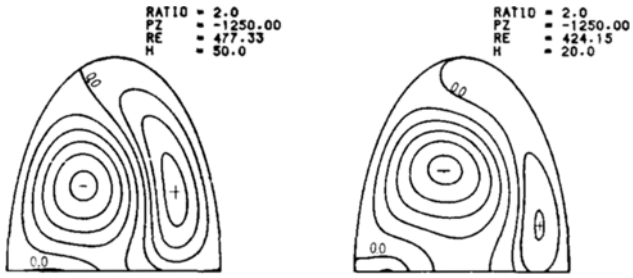

(b) Aspect ratio λ=2.0

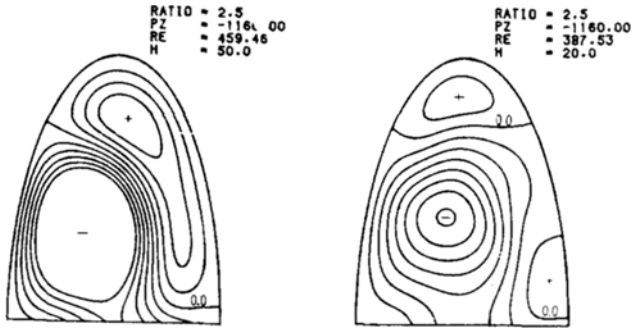

(c) Aspect ratio λ=2.5

Fig.12 Iso-W Contours

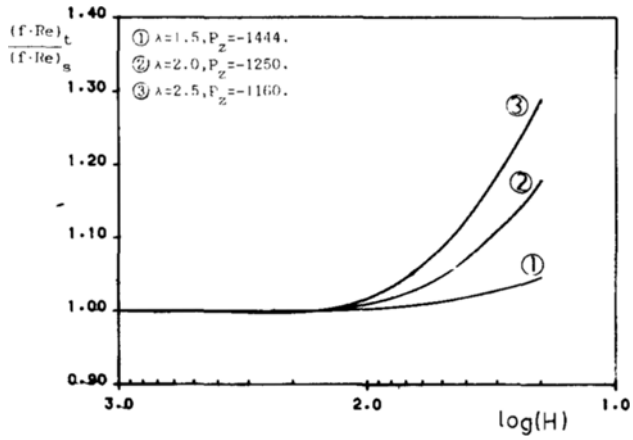

Fig.13 The scaled resistance coefficient $f \cdot Re$

the tube perimeter and counter-balances the pressure force. The so called resistance coefficient $f \cdot Re$ is then given by

$$f \cdot Re = -\frac{\langle P_z \rangle}{\langle V_z \rangle} \cdot \frac{4\lambda}{(1+\lambda)} \tag{18}$$

where the pressure gradient P_z is defined along the helical curve of constant (x, y) in the moving coordinate system.

To calculate mean velocity over a cross-section, the change of variables technique explained by Davis and Rabinowitz (1975) is used. In Fig. 13 it can be observed from the curves of the resistance coefficient (scaled by that of the straight tube) that as the the twist ratio increases, the energy loss also increases rapidly.

5. CONCLUSION

The numerical method developed in the present paper has effectively treated the complicated flow through a twisted elliptic tube. The tube twist ratio and the aspect ratio of the ellipse have indeed been proved to play a significant role in the flow patterns.

The secondary flow lagged behind the winding motion of the potential flow in the twisted tube with large value of twist ratio and small cross-sectional aspect ratio. On the other hand, the secondary flow accelerated beyond the twisting rate of the potential flow for comparatively small tube twist ratio and large aspect ratio of ellipse.

For small twist-ratio tubes, the present solution showed good agreement with the small-parturtation solution presented by Todd.

REFERENCES

Date, A.W., 1974 "Prediction of Fully Developed Flow in a Tube Containing a Twisted Tape", Int. J. Heat Mass Transfer, Vol. 17 pp. 845~859.

Davis, P.J. and Rabinowitz. P., 1975, "Methods of Numerical Integration", Academic Press.

Lopina, R.F. and Bergles, A.E., 1969, "Heat Transfer and Pressure Drop in Tap-Generated Swirl Flow of Single-Phase Water," "ASME Journal of Heat Transfer, Vol. 91, pp. 434~442.

Masliyah, J.H. and Nandakumar, K., 1981a, "Steady Laminar Flow Through Twisted Pipes; Fluid Flow in Square Tubes," ASME Journal of Heat Transfer, Vol. 103, pp. 785~790.

Masliyah, J.J. and Nandakumar, K., 1981b. "Steady Laminar Flow Through Twisted Pipes; Heat Transfer in Square Tubes," ASME Journal of Heat Transfer, Vol. 103, pp. 791~796.

Rohsenow, W.M. and Hartnett J.P., 1973 "Handbook of Heat Transfer", Mc Graw-Hill.

Todd, L., 1977, "Some Comments on Steady, Laminar Flow Through Twisted Pipes," J. of Engineering Mathematics, Vol. 11, pp. 29~48.

APPENDIX

The governing equations in the computational domain (ξ, η, ζ) are as follows:

x-direction momentum equation:

$$P_x=\left[\left(\frac{\partial\xi}{\partial x}\right)\{-V_x-\left(\frac{\pi}{H}\right)V_z\eta-\left(\frac{\pi}{H}\right)^2\xi l\}+\left(\frac{\partial\xi}{\partial y}\right)\{-V_y-\left(\frac{\pi}{H}\right)V_z\xi l-\left(\frac{\pi}{H}\right)^2\eta\}+\left(\frac{\partial^2\xi}{\partial x\partial y}\right)\{-\left(\frac{\pi}{H}\right)^2 2\xi\eta l\}+\left(\frac{\partial^2\xi}{\partial y^2}\right)\{1+\left(\frac{\pi}{H}\right)^2\xi^2 l^2\}\right]\frac{\partial V_x}{\partial\xi}+\{-V_y+\left(\frac{\pi}{H}\right)V_z\xi l-\left(\frac{\pi}{H}\right)^2\eta\}\frac{\partial Vx}{\partial\eta}+\left[\left(\frac{\partial\xi}{\partial x}\right)^2\{1+\left(\frac{\pi}{H}\right)^2\eta^2\}+\left(\frac{\partial\xi}{\partial y}\right)\left(\frac{\partial\xi}{\partial x}\right)\{-\left(\frac{\pi}{H}\right)^2 2\xi\eta l\}+\left(\frac{\partial\xi}{\partial y}\right)^2\{1+\left(\frac{\pi}{H}\right)^2\xi^2 l^2\}\right]\frac{\partial^2 V_x}{\partial\xi^2}+\left[\left(\frac{\partial\xi}{\partial x}\right)\{-\left(\frac{\pi}{H}\right)^2\cdot 2\xi\eta l\}+2\left(\frac{\partial\xi}{\partial\eta}\right)\{1+\left(\frac{\pi}{H}\right)^2\xi^2 l^2\}\right]\frac{\partial^2 V_x}{\partial\xi\partial\eta}+\{1+\left(\frac{\pi}{H}\right)^2\xi^2 l^2\}\frac{\partial^2 V_x}{\partial\eta^2}+\left[\left(\frac{\partial\xi}{\partial x}\right)\{-2\eta\left(\frac{\pi}{H}\right)^2\}+\left(\frac{\partial\xi}{\partial y}\right)\{2\xi l\left(\frac{\pi}{H}\right)^2\}\right]\frac{\partial V_y}{\partial\xi}+\{2\xi l\left(\frac{\pi}{H}\right)^2\}\frac{\partial V_y}{\partial\eta}+\left(\frac{\pi}{H}\right)V_z V_y-\left(\frac{\pi}{H}\right)^2 V_x \quad \text{(A-1)}$$

y-direction momeutum equation:

$$P_y=\left[\left(\frac{\partial\xi}{\partial x}\right)\{-V_x-\left(\frac{\pi}{H}\right)V_z\eta-\left(\frac{\pi}{H}\right)^2\xi l\}+\left(\frac{\partial\xi}{\partial y}\right)\{-V_y-\left(\frac{\pi}{H}\right)V_z\xi l-\left(\frac{\pi}{H}\right)^2\eta\}+\left(\frac{\partial^2\xi}{\partial x\partial y}\right)\{-\left(\frac{\pi}{H}\right)^2 2\xi\eta l\}+\left(\frac{\partial^2\xi}{\partial y^2}\right)\{\left(1+\left(\frac{\pi}{H}\right)^2\xi^2 l^2\right\}\right]\frac{\partial V_y}{\partial\xi}+\{-V_y+\left(\frac{\pi}{H}\right)V_z\xi l-\left(\frac{\pi}{H}\right)^2\eta\}\frac{\partial V_y}{\partial\eta}+\left[\left(\frac{\partial\xi}{\partial y}\right)^2\{1+\left(\frac{\pi}{H}\right)^2\eta^2\}+\left(\frac{\partial\xi}{\partial y}\right)\left(\frac{\partial\xi}{\partial x}\right)\times\{-\left(\frac{\pi}{H}\right)^2 2\xi\eta l\}+\left(\frac{\partial\xi}{\partial y}\right)^2\{1+\left(\frac{\pi}{H}\right)^2\xi^2 l^2\}\right]\frac{\partial^2 V_y}{\partial\xi^2}+\left[\left(\frac{\partial\xi}{\partial x}\right)\{-\left(\frac{\pi}{H}\right)^2\cdot 2\xi\eta l\}+2\left(\frac{\partial\xi}{\partial y}\right)\{1+\left(\frac{\pi}{H}\right)^2\xi^2 l^2\}\right]\frac{\partial^2 V_y}{\partial\xi\partial\eta}+\{1+\left(\frac{\pi}{H}\right)^2\xi^2 l^2\}\frac{\partial^2 V_y}{\partial\eta^2}-\left[\left(\frac{\partial\xi}{\partial x}\right)\{-2\eta\left(\frac{\pi}{H}\right)^2\}+\left(\frac{\partial\xi}{\partial y}\right)\{2\xi l\left(\frac{\pi}{H}\right)^2\}\right]\frac{\partial V_x}{\partial\xi}-\{2\xi l\left(\frac{\pi}{H}\right)^2\}\frac{\partial V_x}{\partial\eta}-\left(\frac{\pi}{H}\right)V_z V_x-\left(\frac{\pi}{H}\right)^2 V_y \quad \text{(A-2)}$$

z-direction momentum equation:

$$-P_z-\frac{\pi}{H}(\eta P_x-\xi l P_y)+\left[\left(\frac{\partial\xi}{\partial x}\right)\{-V_x-\left(\frac{\pi}{H}\right)V_z\eta-\left(\frac{\pi}{H}\right)^2\xi l\}+\left(\frac{\partial\xi}{\partial y}\right)\{-V_y-\left(\frac{\pi}{H}\right)V_z\cdot\xi l-\left(\frac{\pi}{H}\right)^2\eta\}+\left(\frac{\partial^2\xi}{\partial x\partial y}\right)\{-\left(\frac{\pi}{H}\right)^2 2\xi\eta l\}+\left(\frac{\partial^2\xi}{\partial y^2}\right)\{1+\left(\frac{\pi}{H}\right)^2\xi^2 l^2\}\right]\frac{\partial V_z}{\partial\xi}+\{-V_y+\left(\frac{\pi}{H}\right)V_z\xi l-\left(\frac{\pi}{H}\right)^2\eta\}\frac{\partial V_z}{\partial\eta}+\left[\left(\frac{\partial\xi}{\partial x}\right)^2\{1+\left(\frac{\pi}{H}\right)^2\xi^2 l^2\}+\left(\frac{\partial\xi}{\partial y}\right)\left(\frac{\partial\xi}{\partial x}\right)\{-\left(\frac{\pi}{H}\right)^2 2\xi\eta l\}+\left(\frac{\partial\xi}{\partial y}\right)^2\{1+\left(\frac{\pi}{H}\right)^2\xi^2 l^2\}\right]\frac{\partial^2 V_z}{\partial\xi^2}+\left[\left(\frac{\partial\xi}{\partial x}\right)\{-\left(\frac{\pi}{H}\right)^2 2\xi\eta l\}+2\left(\frac{\partial\xi}{\partial y}\right)\{1+\left(\frac{\pi}{H}\right)^2\xi^2 l^2\}\right]\frac{\partial^2 V_z}{\partial\xi\partial\eta}+\{1+\left(\frac{\pi}{H}\right)^2\xi^2 l^2\}\frac{\partial^2 V_z}{\partial\eta^2}=0 \quad \text{(A-3)}$$

Stream-function equation:

$$\left(\frac{\partial^2\xi}{\partial y^2}\right)\frac{\partial\psi}{\partial\xi}+\{\left(\frac{\partial\xi}{\partial x}\right)^2+\left(\frac{\partial\xi}{\partial y}\right)^2\}\frac{\partial^2\psi}{\partial\xi^2}+2\left(\frac{\partial\xi}{\partial y}\right)\frac{\partial^2\psi}{\partial\xi\partial\eta}+\frac{\partial^2\psi}{\partial\eta^2}=\left(\frac{\pi}{H}\right)\left[2V_z+\{\left(\frac{\partial\xi}{\partial x}\right)\xi l+\left(\frac{\partial\xi}{\partial y}\right)\eta\}\frac{\partial V_z}{\partial\xi}+\eta\frac{\partial V_z}{\partial\eta}\right]-\omega_z \quad \text{(A-4)}$$

Vorticity transport equation:

$$\left[\left(\frac{\partial\xi}{\partial x}\right)\{\frac{\partial\psi}{\partial y}+\left(\frac{\pi}{H}\right)^2\xi l\}+\left(\frac{\partial\xi}{\partial y}\right)\{-\frac{\partial\psi}{\partial x}+\left(\frac{\pi}{H}\right)^2 y\}+\left(\frac{\partial^2\psi}{\partial y^2}\right)\{-1-\left(\frac{\pi}{H}\right)^2\xi^2 l^2\}+\left(\frac{\partial^2\xi}{\partial x\partial y}\right)\{\left(\frac{\pi}{H}\right)^2 2\xi\eta l\}\right]\frac{\partial\omega_z}{\partial\xi}+\{-\frac{\partial\psi}{\partial x}+\left(\frac{\pi}{H}\right)^2\eta\}\frac{\partial\omega_z}{\partial\eta}+\left(\frac{\pi}{H}\right)\left(\xi l\frac{\partial V_z}{\partial y}-\eta\frac{\partial V_z}{\partial x}\right)\cdot\omega_z+\left[\left(\frac{\partial\xi}{\partial x}\right)^2\{-1-\left(\frac{\pi}{H}\right)^2\eta^2\}+\left(\frac{\partial\xi}{\partial y}\right)^2\{-1-\left(\frac{\pi}{H}\right)^2\xi^2 l^2\}+\left(\frac{\partial\xi}{\partial y}\right)\left(\frac{\partial\xi}{\partial x}\right)\{2\xi\eta l\left(\frac{\pi}{H}\right)^2\}\right]\frac{\partial^2\omega_z}{\partial\xi^2}+\left[2\left(\frac{\partial\xi}{\partial y}\right)\{-1-\left(\frac{\pi}{H}\right)^2\xi^2 l^2\}+\left(\frac{\partial\xi}{\partial x}\right)\{2\left(\frac{\pi}{H}\right)^2\xi\eta l\}\right]\frac{\partial^2\omega_z}{\partial\xi\partial n}+\{-1-\left(\frac{\pi}{H}\right)^2\xi^2 l^2\}\frac{\partial^2\omega_z}{\partial\eta^2}=-\left(\frac{\pi}{H}\right)\left[\left\{\left(\frac{\partial\xi}{\partial x}\right)\eta-\left(\frac{\partial\xi}{\partial y}\right)\xi l\right\}\frac{\partial V_y}{\partial\xi}-x\frac{\partial V_y}{\partial\eta}+V_x\right]\left(\frac{\partial\xi}{\partial x}\right)\frac{\partial V_z}{\partial\xi}+\left(\frac{\pi}{H}\right)\left[\left\{\left(\frac{\partial\xi}{\partial x}\right)\eta-\left(\frac{\partial\xi}{\partial y}\right)\xi l\right\}\frac{\partial V_x}{\partial\xi}-x\frac{\partial V_x}{\partial\xi}-x\frac{\partial V_x}{\partial\eta}-V_y\right]\left\{\left(\frac{\partial x}{\partial y}\right)\frac{\partial V_z}{\partial\xi}+\frac{\partial V_z}{\partial\eta}\right\} \quad \text{(A-5)}$$